Published online 10 March 2009

Nucleic Acids Research, 2009, Vol. 37, No. 9 ***2789–2795***
doi:10.1093/nar/gkp134

Direct demonstration and quantification of long-range DNA looping by the λ bacteriophage repressor

Chiara Zurla[1], Carlo Manzo[1], David Dunlap[2], Dale E. A. Lewis[3], Sankar Adhya[3] and Laura Finzi[1,*]

[1]Physics Department, 400 Dowman Dr., [2]Cell Biology Department, 615 Michael St, Emory University, Atlanta, GA 30322 and [3]Laboratory of Molecular Biology, NCI, NIH, 37 Convent Drive, Bethesda, MD 20892-4264, USA

Received September 23, 2008; Revised February 13, 2009; Accepted February 17, 2009

ABSTRACT

Recently, it was proposed that DNA looping by the λ repressor (CI protein) strengthens repression of lytic genes during lysogeny and simultaneously ensures efficient switching to lysis. To investigate this hypothesis, tethered particle motion experiments were performed and dynamic CI-mediated looping of single DNA molecules containing the λ repressor binding sites separated by 2317 bp (the wild-type distance) was quantitatively analyzed. DNA containing all three intact operators or with mutated *o3* operators were compared. Modeling the thermodynamic data established the free energy of CI octamer-mediated loop formation as 1.7 kcal/mol, which decreased to –0.7 kcal/mol when supplemented by a tetramer (octamer+tetramer-mediated loop). These results support the idea that loops secured by an octamer of CI bound at *oL1, oL2, oR1* and *oR2* operators must be augmented by a tetramer of CI bound at the *oL3* and *oR3* to be spontaneous and stable. Thus the *o3* sites are critical for loops secured by the CI protein that attenuate *cI* expression.

INTRODUCTION

From viruses to humans, transcription is regulated by proteins that bind to DNA. It is becoming increasingly clear that, in most cases, genes are controlled by large, cooperative assemblages of proteins that wrap and loop the DNA. These protein-induced DNA conformational changes can constitute functional 'epigenetic switches' in which alternative configurations commit the system to one developmental pathway or another. Such is the case of temperate bacteriophages which exhibit either quiescent (lysogenic) or productive (lytic) growth. The classic epigenetic switch found in bacteriophage λ is not only a paradigm of transcriptional regulation, but is also at the basis of our understanding of phage lysogeny (1). The latter is relevant to the investigation of uses of phages as antibacterial agents and phage therapy (2–4), and to the control of several infectious diseases. Indeed, bacteriophages contribute to the virulence of many bacterial pathogens, largely by encoding the structural genes for virulence factors (5–8). Prophage induction and phage-mediated lysis can contribute to production and release of virulence factors from bacterial cells (9,10) which cause a wide range of diseases (7–12).

Our understanding of phage lysogeny is based primarily on the detailed information about the λ bacteriophage (13). Lysogeny may ensue after infection, if a repressor protein binds to multipartite operators and mediates cooperative, long-range interactions to repress the lytic genes and maintain a stable lysogenic state. Subsequently, adverse environmental conditions (DNA damage, poisoning, starvation, etc.) can trigger a cascade of events that leads to repressor inactivation and efficient switch to lysis. The lysogenic state of λ prophages is maintained by the λ repressor (CI). During lysogeny, dimers of CI bind to the *oL* and *oR* control regions, located about 2.3 bp apart on the phage genome and repress the *pL* and *pR* promoters of the lytic genes. Each control region contains three binding sites for CI, *oL1*, *oL2*, *oL3* and *oR1*, *oR2*, *oR3* (14). CI binds to these operators with an intrinsic affinity $oL1 > oR1 > oL3 > oL2 > oR2 > oR3$ (15,16). When bound to adjacent or nearby operators, pairs of dimers interact forming tetramers. These cooperative interactions improve the specificity and strength of CI binding, so that CI affinity varies as follows: $oR1 \sim oL1 \sim oR2 \sim oL2 > oL3 > oR3$. Occupancy of *oR2* by CI also activates transcription of the CI gene from

*To whom correspondence should be addressed. Tel: +1 (404) 727 4930; Fax: +1 (404) 727 0873; Email: lfinzi@emory.edu

The authors wish it to be known that, in their opinion, the first two authors should be regarded as joint First Authors.

the *pRM* promoter (17) to boost the amount of CI and favor the lysogenic state.

However, CI overexpression is regulated to avoid high concentrations that would obstruct efficient switching to lysis when necessary. Long-range DNA-looping between CI-bound operators *oR* and *oL* has been proposed to be critical for this regulation (18–20). DNA loops of 2850 bp have been demonstrated *in vitro* using electron microscopy, and the presence of the *oL* operator at 3.6-bp separation was shown to improve CI repression of the lytic *pR* promoter *in vivo* (18). Improved repression of *pR* in the presence of *oL*, expected to stabilize lysogeny, was confirmed in subsequent studies (20,21). Biophysical and structural studies (22–25) support the idea of Dodd and collaborators (20) that CI tetramers bound at *oL1* and *oL2* and at *oR1* and *oR2* can pair to form a CI octamer, which secures a loop of intervening DNA and juxtaposes the *oL3* and *oR3* operators. In this arrangement, a CI dimer bound at the strong *oL3* site could coordinate with another bound to the weak *oR3* site, forming a tetramer that would further secure the DNA loop (Supplementary Data, Figure S1). Such loop-driven cooperativity would favor *oR3* occupancy at physiological CI concentrations to prevent CI overexpression from *pRM*, which would interfere with rapid switching from lysogeny to lysis (19,20). This model is based on *in vivo* experiments that show a strong dependence of *pRM* repression on the distant (3.6–3.8-bp separation) CI-binding sites at *oL* (19,20,26). Therefore in λ, DNA looping is thought to maximally attenuate transcription from *pR* and *pL*, achieve repression of *pRM*, and enables efficient switching to lysis from the lysogenic state.

Nonetheless, direct evidence for looping has been obtained only by electron microscopy, precluding observation of reversible looping dynamics, and only allowing observation of the presumed octamer-mediated loop (18). Model-based analyses of *in vivo* transcription data (20,26) have provided estimates of the energy for the formation of a CI octamer-mediated loop and for the tetramerization of CI bound to the *o3* sites juxtaposed by the DNA loop. Here, we used the tethered particle motion (TPM) technique (27–30) to demonstrate dynamic, long-range CI-mediated DNA looping *in vitro*. The free energies of formation of CI octamer- and octamer + tetramer-mediated loops were measured using DNA with either wild-type or mutationally disrupted *o3* operators. Modeling the manifold configurations quantified how a CI octamer-mediated loop is stabilized by an adjunct CI tetramer to give an 'octamer + tetramer' secured loop (20,26).

MATERIALS AND METHODS

Plasmids

The TPM measurements were performed on DNA derived from plasmids pDL2317 (wt λ DNA), pDL*ΔoL* 2317 (λ*ΔoL* DNA), pDL2320 (λ*o3*$^-$ DNA) and pDL2321 (λ*oL*$^-$*oR*$^-$ DNA). To obtain plasmid pDL2317, which contains the complete λ regulatory region, a 2028-bp fragment from bacteriophage λ DNA (New England Biolabs GmbH, Frankfurt am Main, Germany) was amplified using primers phageEcoRI, 5′-ttctgctttgaattctgcccttcttca gggcttaatttttaagagcgtcaccttcatgg-3′, and lambdaAVRI, 5′-tataacgccgcctaggttgcaaaaattctcaaagttagcgttgaagaatttag ccc-3′. This fragment was then inserted between the BglII and AvrII restriction sites of plasmid pDL300 (27). To obtain plasmid pDL*ΔoL* 2317, a 329-bp fragment from pDL*ΔoL1-2-3* (27) was amplified using primers BioC 5′-cgcaattaatgtgagttagctcactcattaggcaccccaggc-3′ and lambda Avr-BglR 5′-ctaggttgcaaaaattagatctctcacctaccaaa caatgccccctgcaaaaaataaattcatataaaaaacatacag-3′, and inserted between the EcoRI and BglII restriction sites of pDL2317.

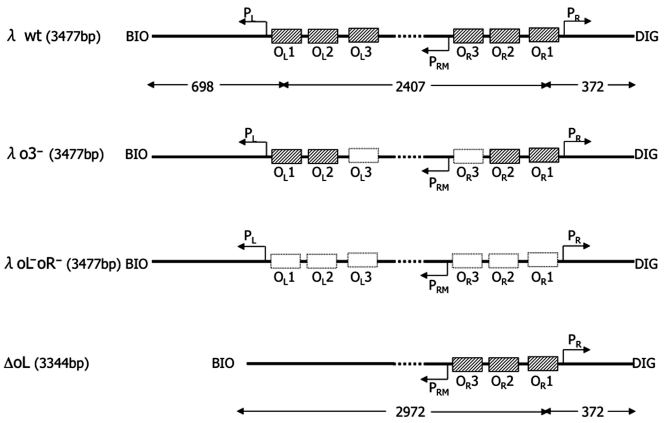

Figure 1. DNA constructs used. Name and overall length are indicated next to each fragment. The length of the different parts of the fragments is indicated below the first and last fragment. The biotin (BIO) and digoxigenin (DIG) labels used to anchor the DNA molecules to the glass and bead surfaces are indicated at each end of the fragments. P_L and P_R are the two lytic promoters, while P_{RM} is the promoter for *cI* transcription. The rectangular, shaded boxes on the DNA indicate the operators where CI binds specifically. The white boxes indicate the mutated operators.

To obtain plasmids pDL2320 and pDL2321, a 2156-bp-long fragment from bacteriophage λ DNA was amplified using primers lambdaBglII, 5′-caggggggcattgttt ggtaggtgagagatcttgaattgctatgtttagtgagttgtatc-3′ and lambda AvrIIbis, 5′-tataacgccgcctaggaaagaaaaatgaacttgg cttatcccaggaatctgtcgcagacaagatggg3′. The product was cloned between the BglII and AvrII restriction sites in pDL965, which carries point mutations in the operators *oL3* and *oR3*, and pDL970 which instead has point mutations in all the *oL* and *oR* binding sites (Lewis *et al.*, manuscript in preparation). Since known mutations are leaky and pleiotropic, mutations r1 (7C to T, found in *oR3*) and v1 (6C to A, found in *oR2*) (17,31,32) were combined to eliminate CI binding. The DNA fragments for TPM, that are schematically represented in Figure 1, were obtained by PCR on templates pDL2317, pDL*Δo*L 2317, pDL2320 and pDL2321 in the presence of a biotin-labeled primer 5′-cgcaattaatgtgagttagctcactcattaggcaccccaggc-3′ and a digoxigenin-labeled primer 5′-gcattgcttatcaatttgttgc aacgaacaggtcactatcagtc-3′ (Oligos etc. Inc., OR, USA). In each fragment, except for λ*ΔoL* DNA, the *oL* and *oR* regulatory regions are separated by 2317 bp. All unmodified primers were purchased from Sigma Genosys (the Woodlands, TX, USA).

Table 1. Thermodynamic parameters

Operator	$\triangle G$ (kcal/mol)	Operator	$\triangle G$ (kcal/mol)	Parameter (units)	Value
oL1[a]	–13.0	*oR1*[b]	–12.5	$\triangle G_{NS}$[d] (kcal/mol)	–4.1
oL2[a]	–11.2	*oR2*[b]	–10.5	$\triangle G_{D}$[e] (kcal/mol)	–11.1
oL3 wt[a] (*o3*$^-$)[c]	–12.0 (–4.1)	*oR3* wt[b] (*o3*$^-$)[c]	–9.5 (–4.1)	[DNA] (M)	$<1{\cdot}10^{-12}$
oL1-oL2 coop[a]	–2.7	*oR1-oR2* coop[b]	–2.7	l (bp)	3477
oL1-oL3 coop[a]	0	*oR1-oR3* coop[b]	0	$\triangle G_{oct}$[f] (kcal/mol)	1.7
oL2-oL3 coop[a]	–2.0	*oR2-oR3* coop[b]	–2.9	$\triangle G_{tetr}$[f] (kcal/mol)	–2.4

The table reports the DNA length and the thermodynamic parameters used in the fitting, and the free energy obtained for octamer-mediated loop formation and for subsequent tetramer formation.
[a]From calculations by Anderson and Yang, based on data by Senear *et al.* (16).
[b]From Koblan and Ackers (15).
[c]Affinities for the binding to the point-mutated operators *o3*$^-$ (value in parentheses) are set as equal to the nonspecific binding (26,35,37).
[d]Nonspecific binding affinity at 200 mM KCl from Bakk and Metzler (35,37).
[e]CI dimerization free energy at 200 mM KCl from Koblan and Ackers (36).
[f]Results of the performed analysis (Figure 3).

Tethered particle motion experiments

Tethered particle motion assays. Details of the TPM technique have been published previously (27,29,30,33,34), and Figure 2 schematically illustrates the technique. In brief, a submicron-size bead is tethered by a single DNA molecule to the glass surface of a microscope flow-chamber. The mobile end of the invisible DNA is marked by the bead which exhibits Brownian motion that is constrained by the DNA tether length. Thus if the DNA undergoes a conformational change, such as loop formation, which reduces the effective tether length, the Brownian excursions of the bead will diminish. Stochastic, protein-mediated, DNA loop formation and breakdown will generate a telegraphic-like TPM signal in time.

Four to six antidigoxigenin-coated beads (480 nm; Indicia Diagnostics, Oullins, France) were tracked in each microchamber in λ buffer (10 mM Tris–HCl pH 7.4, 200 mM KCl, 5% DMSO, 0.1 mM EDTA, 0.2 mM DTT and 0.1 mg/ml α-casein) for ~10 min. CI protein was added in the same buffer and tracking was continued for ~30 min. The procedure was repeated in order to monitor the motion of 50 to 100 DNA-tethered beads for each CI concentration. The square modulus of the projected displacement vector $\rho^2(t) = x(t)^2 + y(t)^2$ was calculated from the drift-corrected $x(t)$ and $y(t)$ as described (29). The 4-s moving average of the filtered time series, $\sqrt{\langle\rho^2(t)\rangle_{4s}}$, produced traces such as those shown in Figure 3. The $\sqrt{\langle\rho^2(t)\rangle_{4s}}$ values obtained in the control experiments (no CI, ~375 nm) and those corresponding to the looped state in the presence of CI (~225 nm) were as expected from a published calibration curve (29) (Supplementary Data, Figure S2). Cumulative histograms of all the TPM data points were plotted and a Gaussian distribution was used to fit the data corresponding to the looped configuration of DNA (Figure 4). The loop probability was calculated as the ratio between the area under the Gaussian curve and the total area of the histogram. The uncertainties of the measured loop probability were determined by error propagation of the 68% confidence interval of the Gaussian fitting parameters.

CI concentrations. The estimated lysogenic concentration of CI is roughly 52 nM/prophage, assuming an average multiplicity of four chromosomes per cell (35). Thus we performed measurements between 20 and 170 nM. Data obtained at any higher concentrations were not interpretable due to nonspecific CI binding which produced an intermediate range of tether lengths (see 'Discussion' section). On the other hand, the frequency of loop formation below 20 nM was so low that statistically significant data could not be collected.

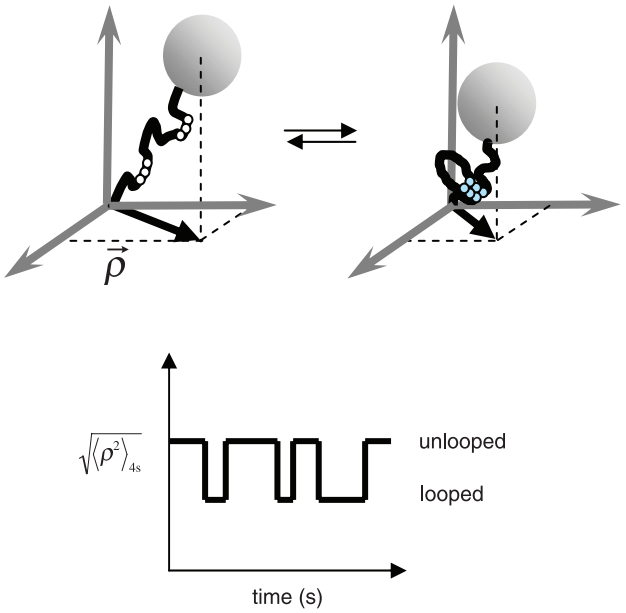

Figure 2. Schematics of the TPM experiment using a λ DNA tether. The six operators are indicated as white circles along the DNA. Dimers of CI bound to operators (cyan circles) can interact forming a DNA loop. The change in DNA length is recorded as a change in TPM signal, $\sqrt{\langle\rho^2\rangle_{4s}}$, versus time.

Thermodynamic modeling

In order to relate the measured loop probabilities to the microscopic configurations of CI bound to the six operator sites, 81 unlooped and 32 looped configurations were

considered according to Anderson and Yang (26). The probability for each DNA–protein configuration was expressed as,

$$f_s = \frac{[CI_2]^{i_s} \exp(-\Delta G_s/RT)}{\sum_s [CI_2]^{i_s} \exp(-\Delta G_s/RT)} \quad \mathbf{1}$$

where ΔG_s is the sum of the free energies for binding, short-range cooperativity and looping of each configuration and i_s is the number of bound CI dimers. CI dimer concentration was calculated from the expression for the total concentration of CI:

$$[CI]_{tot} = \sqrt{\frac{[CI_2]}{K_d}} + 2[CI_2] + 2K_{NS}l[DNA][CI_2] + [DNA]\sum_s i_s f_s \quad \mathbf{2}$$

where K_d is the dimerization constant for CI (36), K_{NS} is the nonspecific binding constant (37), and l is the DNA length in base pairs (Table 1). The terms of this equation represent: CI monomers, CI dimers, nonspecifically bound and specifically bound CI.

The concentration-dependent loop probability was then calculated as,

$$\text{loop probability} = \frac{\sum_{s=82}^{113} f_s}{\sum_{s=1}^{113} f_s} \quad \mathbf{3}$$

The free energy for each unlooped species was expressed as the sum of all the ΔGs for binding and short-range cooperativity. The free energy expression for the looped species also included the term ΔG_{oct}, and the tetramerization term ΔG_{tetr} was added only for the configuration in which two CI dimers not involved in the octamer were juxtaposed (26). Using this model, the probability of looping was expressed as a function of CI concentration. The experimental data obtained using both wt λ and $\lambda o3^-$ DNA were fitted simultaneously to estimate ΔG_{oct} and ΔG_{tetr} using custom Matlab routines based on the *fminsearch* function.

RESULTS AND DISCUSSION

The motion of several hundred DNA-tethered beads was monitored in the presence of CI concentrations varying from 0 to 170 nM. This titration was performed on two different DNA fragments: the wt λ and the $\lambda o3^-$ DNA. $\lambda o3^-$ DNA carries double-point mutations in the *oL3* and *oR3* sequences. These mutations abrogate the binding of CI to both these sites and, therefore, should prevent formation of loops mediated by more than a CI octamer.

In the absence of protein (Figure 3, upper panel) the TPM signal, $\sqrt{\langle \rho^2 \rangle_{4s}}$, was constant. In fact, all unlooped tethers in the absence of protein exhibited a narrow range of extensions as shown in the cumulative histograms for the controls of each condition (Figure 4, gray distributions, and Supplementary Data Figure S4). In the presence of CI the TPM signal transiently dropped to a lower level

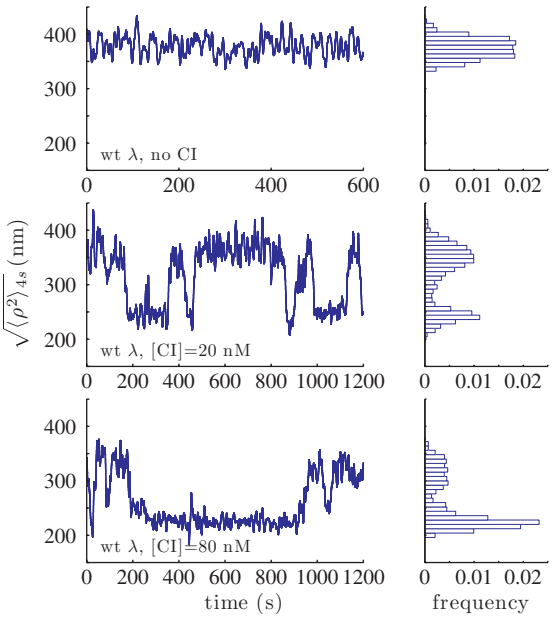

Figure 3. $\sqrt{\langle \rho^2 \rangle_{4s}}$ as a function of time for beads tethered by a 3477-bp DNA fragment containing the *oL-oR* regulatory regions separated by 2317 bp (wt λ DNA): (upper) In the absence of CI (control), (middle) In the presence of 20 nM, and (lower) 80 nM CI. Frequency histograms, corresponding to the individual TPM traces, are shown to the left. The histograms are normalized to the total number of events and to the bin width (8 nm).

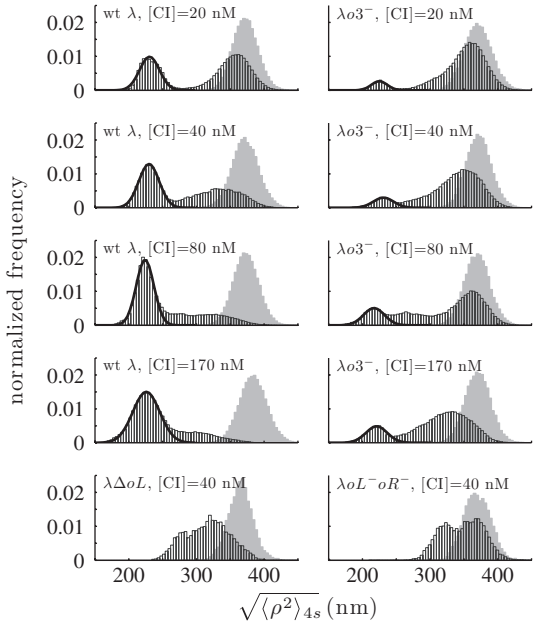

Figure 4. Frequency histograms of the distribution of $\sqrt{\langle \rho^2 \rangle_{4s}}$ (Left): wt λ DNA in the presence of 20, 40, 80 and 170 nM CI; (lower left): λ△*oL* DNA in the presence of 40 nM CI; (right): $\lambda o3^-$ DNA at 20, 40, 80 and 170 nM CI; (lower right): λoL^-oR^- DNA with 40 nM CI. The histograms are normalized to the total number of events and to the bin width (4 nm). The solid lines show the results of fitting by a Gaussian distribution. The gray distributions are those of the control measurements performed in the absence of CI previous to each experimental condition.

that corresponded to the effective length of the looped DNA, as expected from a simple length-loss model [see calibration curve, Supplementary Data Figure S2 (29)]. The middle and lower panels of Figure 3 show representative traces recorded at 20 and 80 nM CI along with corresponding histograms. Clearly the stability and probability of loops increased as the concentration of CI increased. These observations were confirmed by the cumulative histograms of all the measurements performed at various CI concentrations (Figure 4, four upper left panels), which display a peak centered on 225 nm, corresponding to the looped DNA. Gaussians fitted to the 'looped' peak as well as the control (no protein) peak showed little variations across all experimental conditions (Supplementary Data, Figure S3). In both cases the data lie within 10 nm of the average value, which is within the resolution of TPM (indicated by dotted lines). The peak at 225 nm did not appear using either $\lambda oL^{-}oR^{-}$ DNA in which all six operators were mutated to abrogate CI binding (Figure 4, lower right) or $\lambda\Delta oL$ DNA in which the *oL* but not the *oR* region had been deleted (Figure 4, lower left).

Figure 4 also shows that the distribution of the unlooped state broadened as CI concentration increased and the mean shifted toward smaller values, suggesting that nonspecific CI binding may loop or bend the DNA to shorten the tethers. The probability of formation of a semispecific loop was determined as the probability of nonspecific binding at a distance L_{NS} from the specific operators multiplied by the circularization factor $J(L_{NS})$. The probability for nonspecific binding is not length dependent, while *J* can be calculated by means of statistical models (38,39) and shows a maximum for loops of 400–450 bp. Such a loop would only reduce the TPM signal, shifting the distribution maximum to 345 nm. However, two semispecific (or nonspecific) loops would be expected to reduce the corresponding TPM signal to about 325 nm (Supplementary Data, Figure S4). CI binding to both $\lambda\Delta oL$ and $\lambda oL^{-}oR^{-}$ DNA produces a peak at this value. While interesting from a biophysical point of view, these forms are not expected to be important transcriptionally and are completely distinct from the loop mediated by specifically bound CI. It is also possible that nonspecific and specific binding bend DNA similarly (40), and that bends from multiple, nonspecifically bound CI proteins produce the intermediate signals (currently under investigation). In either case, these forms do not obscure specific looping in our data.

Loops formed in both the wt λ and the $\lambda o3^{-}$ DNA, although less frequently in the latter case (Figure 4, upper four right panels). These observations confirmed that the presence of two operators at *oL* and *oR* suffices to permit a low level of loop formation and that the *o3* sites shift the equilibrium toward looping. A structural study of CI by Stayrook *et al.* (25) showed that contact is precluded between a cooperatively bound dimer pair at *oR1* and *oR2* and an adjacently bound third dimer at *oR3* (and analogously for dimers bound at *oL1, oL2* and *oL3*). Therefore, the only apparent means of further stabilization of looping by CI dimers bound at the *o3* sites is through head-to-head interactions with the consequent

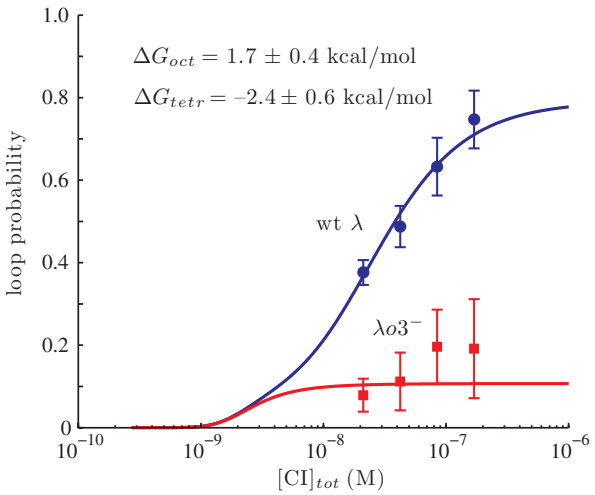

Figure 5. Loop probability as a function of CI concentration for wt λ (dots) and $\lambda o3^{-}$ DNA (squares). The lines are the result of the global simulation performed as explained in the text. Errors on the fitted parameters have been estimated at 95.4% confidence interval using constant χ^2 boundaries as a confidence limit [(45) and Supplementary Data, Figure S5]. $\chi^2 = \Sigma\ [(expected - data)/error)^2] = 3.02$, where *expected* = expected values of the data; *data* = experimentally observed value of the data; *error* = error on the data.

formation of a CI tetramer. The probability of loop formation, calculated as described in the 'Materials and methods' section, is reported in Figure 5. The wt λ DNA spent ~40% of the time in the looped configuration at the lowest CI concentration used (20 nM) and ~80% of the time at the highest concentration (170 nM). In contrast, the $\lambda o3^{-}$ DNA loop probability was ~10% at 20 and 40 nM CI and rose to only ~18% at 170 nM CI (Figures 4 and 5). These values are in agreement with an estimate obtained using EM (12%) on DNA fragments also containing only two pairs of operators (18). A statistical mechanical model, first proposed by Koblan *et al.* (15) and subsequently extended by Dodd *et al* (20) and Anderson and Yang (26), was used to validate the hypothesis that the concentration dependence of loop probability is due to the following two-step mechanism: (i) loop formation via interaction between a pair of CI tetramers bound at the *oL* and *oR* region, leading to a loop secured by a CI octamer (with free energy ΔG_{oct}); and (ii) head-to-head interaction, or tetramer formation, between two CI dimers bound to the remaining operators juxtaposed by the DNA loop (with free energy ΔG_{tetr}), which leads to an increase in loop stability (15,16). Using the configurational possibilities described by Anderson and Yang (26), 81 unlooped and 32 looped configurations were considered (see 'Materials and Methods' section).

All the experimental data obtained using wt λ or $\lambda o3^{-}$ DNA were fitted simultaneously to estimate ΔG_{oct} and ΔG_{tetr} (Figure 5). Since the two mutations in $\lambda o3^{-}$ DNA abrogate specific CI binding, nonspecific DNA dissociation constants in the millimolar range (35,37) were used to model the $o3^{-}$ operators. The resulting model curve for the wt λ looping probability quickly rises with CI concentration, while the $o3^{-}$ curve derived from the fitting

remains near 10% across the range of CI concentrations employed. Remarkably, this fit of the looping titrations for both the *wt* and the mutant $\lambda o3^-$ DNA was obtained with only two free parameters, $\Delta G_{oct} = 1.7 \pm 0.4$ kcal/mol and $\Delta G_{tetr} = -2.4 \pm 0.6$ kcal/mol. It indicates that the *o3* operators are critical for loop stability and their dissociation constants determine loop probability. Notably, the free energy contribution due to the tetramerization reaction is comparable to the value obtained from modeling *in vivo* transcription assays (–3.0 kcal/mol) (20) and to the values reported for *cis* DNA-bound dimmer–dimer interaction (–2 to –3 kcal/mol) (16). ΔG_{oct} is higher than the value obtained in the *in vivo* work by the groups of Dodd and Yang (20,26). This difference is most likely due to the fact that the DNA plasmids used in those measurements were supercoiled, while our DNA tethers were torsionally relaxed (41).

The free energy change associated with the octamer-mediated loop formation can be expressed as the sum of two contributions:

$$\Delta G_{oct} = -RT \log J + \Delta G_{oct}^{(P)}$$

The first term corresponds to the unfavorable free energy change due to bringing the *oL* and the *oR* regions in close proximity (entropic cost of looping), while the second is due to the favorable change resulting from protein–protein interactions. The J factor can be calculated knowing just the persistence length (ξ) of DNA and the separation between the two sites (l_{loop}) (38). The loop is 2317-bp long and, in our experimental conditions, $\xi = 43$ nm (29,42,43). Thus $-RT \log J$ equals 10.2 kcal/mol. From this value and the equation above, the free energy change due to the interaction of the two pairs of dimers involved in the octamer-mediated loop was calculated to be ~–8.5 kcal/mol. This is in good agreement with the free energy change of –9 kcal/mol associated with the interaction of two CI tetramers without DNA, as determined by sedimentation equilibrium experiments (22,24). Hence, while CI is able to octamerize while bound simultaneously to oL and oR, the magnitude of the free energy term from protein–protein interaction is not sufficient to favor loop formation. However, tetramerization between the CI molecules bound to the sites not involved in the octamer-mediated loop (ΔGtetr) lowers the free energy by an additional 2.4 kcal/mol to reverse the sign of the total free energy, rendering loop formation energetically favorable.

In summary, this work provides the first direct evidence that *o1* and *o2* operators suffice for a low level of CI-mediated looping between *oL* and *oR*, which significantly increases when all six operators are functional. This is consistent with a model in which DNA loops mediated by a CI octamer may be further stabilized, in a CI-concentration-dependent manner, by tetramerization of CI bound to a third operator, and strongly supports the idea that the arrangement of λ operators is the minimum required to guarantee robust lysogeny (strong repression of lytic genes) and efficient switching to lysis (repression of *pRM*) at physiological CI levels. In this view, looping is not an evolutionary decoration, but an epigenetic strategy for efficient transcriptional regulation (44). Since λ is not only a paradigm for transcriptional regulation, but also for genetic networks, the thermodynamic underpinnings of this regulatory loop are important to understand both sensitivity and stability of genetic switches.

SUPPLEMENTARY DATA

Supplementary Data are available at NAR Online.

ACKNOWLEDGEMENTS

We wish to thank Ian Dodd for reading our manuscript and providing many useful comments.

FUNDING

HFSPO (RGP0050/2002-C to L.F. and S.A.); Emory URC-2006 (to LF); Intramural Research Program of the National Institutes of Health, National Cancer Institute and the Center for Cancer Research (to S.A.). Funding for open access charge: SA's Intramural Research Program of the National Institutes of Health, National Cancer Institute and the Center for Cancer Research.

Conflict of interest statement. None declared.

REFERENCES

1. Ptashne,M.C.P. (1986) *A Genetic Switch: Gene Control and Phage Lambda*. Cell Press, Cambridge, MA pp. 1.
2. Parisien,A., Allain,B., Zhang,J., Mandeville,R. and Lan,C.Q. (2008) Novel alternatives to antibiotics: bacteriophages, bacterial cell wall hydrolases, and antimicrobial peptides. *J. Appl. Microbiol.*, **104**, 1–13.
3. Waehler,R., Russell,S.J. and Curiel,D.T. (2007) Engineering targeted viral vectors for gene therapy. *Nat. Rev. Genet.*, **8**, 573–587.
4. Projan,S. (2004) Phage-inspired antibiotics? *Nat. Biotechnol.*, **22**, 167–168.
5. Barksdal,L. and Arden,S.B. (1974) Persisting bacteriophage infections, lysogeny, and phage conversions. *Annu. Rev. Microbiol.*, **28**, 265–299.
6. Boyd,E.F. and Brussow,H. (2002) Common themes among bacteriophage-encoded virulence factors and diversity among the bacteriophages involved. *Trends Microbiol.*, **10**, 521–529.
7. Wagner,P.L. and Waldor,M.K. (2002) Bacteriophage control of bacterial virulence. *Infect. Immun.*, **70**, 3985–3993.
8. Wagner,P.L. (2006) In Calender,R. (ed.), *The Bacteriophages*. Oxford University Press, New York, pp. 710–719.
9. Wagner,P.L., Livny,J., Neely,M.N., Acheson,D.W.K., Friedman,D.I. and Waldor,M.K. (2002) Bacteriophage control of Shiga toxin 1 production and release by Escherichia coli. *Mol. Microbiol.*, **44**, 957–970.
10. Wagner,P.L., Neely,M.N., Zhang,X.P., Acheson,D.W.K., Waldor,M.K. and Friedman,D.I. (2001) Role for a phage promoter in Shiga toxin 2 expression from a pathogenic Escherichia coli strain. *J. Bacteriol.*, **183**, 2081–2085.
11. Bensing,B.A., Rubens,C.E. and Sullam,P.M. (2001) Genetic loci of Streptococcus mitis that mediate binding to human platelets. *Infect. Immun.*, **69**, 1373–1380.
12. Bensing,B.A., Siboo,I.R. and Sullam,P.M. (2001) Proteins PblA and PblB of Streptococcus mitis, which promote binding to human platelets, are encoded within a lysogenic bacteriophage. *Infect. Immun.*, **69**, 6186–6192.
13. Ptashne,M. (2004) *A Genetic Switch: Phage Lambda Revisited*, 3rd edn. Cold Spring Harbor Laboratory Press, Cold Spring Harbor, NY pp. 11–29.

14. Maniatis,T. and Ptashne,M. (1973) Multiple Repressor Binding At Operators In Bacteriophage-Lambda — (Nuclease Protection Polynucleotide Sizing Pyrimidine Tracts Supercoils E-Coli). *Proc. Natl Acad. Sci. USA*, **70**, 1531–1535.
15. Koblan,K.S. and Ackers,G.K. (1992) Site-specific enthalpic regulation of DNA-transcription at bacteriophage-lambda Or. *Biochemistry*, **31**, 57–65.
16. Senear,D.F., Brenowitz,M., Shea,M.A. and Ackers,G.K. (1986) Energetics of cooperative protein DNA interactions – comparison between quantitative deoxyribonuclease footprint titration and filter binding. *Biochemistry*, **25**, 7344–7354.
17. Meyer,B.J., Maurer,R. and Ptashne,M. (1980) Gene-regulation at the right operator (Or) of bacteriophage-lambda.2. Or1, Or2, and Or3 - their roles in mediating the effects of repressor and Cro. *J. Mol. Biol.*, **139**, 163–194.
18. Revet,B., von Wilcken-Bergmann,B., Bessert,H., Barker,A. and Muller-Hill,B. (1999) Four dimers of lambda repressor bound to two suitably spaced pairs of lambda operators form octamers and DNA loops over large distances. *Curr. Biol.*, **9**, 151–154.
19. Dodd,I.B., Perkins,A.J., Tsemitsidis,D. and Egan,J.B. (2001) Octamerization of lambda CI repressor is needed for effective repression of P-RM and efficient switching from lysogeny. *Genes Dev.*, **15**, 3013–3022.
20. Dodd,I.B., Shearwin,K.E., Perkins,A.J., Burr,T., Hochschild,A. and Egan,J.B. (2004) Cooperativity in long-range gene regulation by the lambda CI repressor. *Genes Dev.*, **18**, 344–354.
21. Svenningsen,S.L., Costantino,N., Court,D.L. and Adhya,S. (2005) On the role of Cro in lambda prophage induction. *Proc. Natl Acad. Sci. USA*, **102**, 4465–4469.
22. Bandyopadhyay,S., Mukhopadhyay,C. and Roy,S. (1996) Dimer-dimer interfaces of the lambda-repressor are different in liganded and free states. *Biochemistry*, **35**, 5033–5040.
23. Bell,C.E. and Lewis,M. (2001) Crystal structure of the lambda repressor C-terminal domain octamer. *J. Mol. Biol.*, **314**, 1127–1136.
24. Senear,D.F., Laue,T.M., Ross,J.B.A., Waxman,E., Eaton,S. and Rusinova,E. (1993) The primary self-assembly reaction of bacteriophage-lambda Ci repressor dimers is to octamer. *Biochemistry*, **32**, 6179–6189.
25. Stayrook,S., Jaru-Ampornpan,P., Ni,J., Hochschild,A. and Lewis,M. (2008) Crystal structure of the lambda repressor and a model for pairwise cooperative operator binding. *Nature*, **452**, 1022–1026.
26. Anderson,L.M. and Yang,H. (2008) DNA looping can enhance lysogenic CI transcription in phage lambda. *Proc. Natl Acad. Sci. USA*, **105**, 5827–5832.
27. Zurla,C., Franzini,A., Galli,G., Dunlap,D.D., Lewis,D.E.A., Adhya,S. and Finzi,L. (2006) Novel tethered particle motion analysis of CI protein-mediated DNA looping in the regulation of bacteriophage lambda. *J. Phys.-Condens. Matter*, **18**, S225–S234.
28. Finzi,L. and Gelles,J. (1995) Measurement of lactose repressor-mediated loop formation and breakdown in single DNA-molecules. *Science*, **267**, 378–380.
29. Nelson,P.C., Zurla,C., Brogioli,D., Beausang,J.F., Finzi,L. and Dunlap,D. (2006) Tethered particle motion as a diagnostic of DNA tether length. *J. Phys. Chem. B*, **110**, 17260–17267.
30. Pouget,N., Dennis,C., Turlan,C., Grigoriev,M., Chandler,M. and Salome,L. (2004) Single-particle tracking for DNA tether length monitoring. *Nucleic Acids Res.*, **32**, e73.
31. Johnson,A.D., Meyer,B.J. and Ptashne,M. (1979) Interactions between DNA-bound repressors govern regulation by the lambda-phage repressor. *Proc. Natl Acad. Sci. USA*, **76**, 5061–5065.
32. Maurer,R., Meyer,B.J. and Ptashne,M. (1980) Gene-regulation at the right operator (Or) of bacteriophage-lambda.1. Or3 and autogenous negative control by repressor. *J. Mol. Biol.*, **139**, 147–161.
33. Finzi,L. and Dunlap,D. (2003) Single-molecule studies of DNA architectural changes induced by regulatory proteins. *Methods Enzymol.*, **370**, 369–378.
34. Vanzi,F., Broggio,C., Sacconi,L. and Pavone,F.S. (2006) Lac repressor hinge flexibility and DNA looping: single molecule kinetics by tethered particle motion. *Nucleic Acids Res.*, **34**, 3409–3420.
35. Bakk,A. and Metzler,R. (2004) In vivo non-specific binding of lambda CI and Cro repressors is significant. *FEBS Lett.*, **563**, 66–68.
36. Koblan,K.S. and Ackers,G.K. (1991) Energetics of subunit dimerization in bacteriophage-lambda CI repressor-linkage to protons, temperature, and KCL. *Biochemistry*, **30**, 7817–7821.
37. Bakk,A. and Metzler,R. (2004) Nonspecific binding of the O-R repressors CI and Cro of bacteriophage lambda. *J. Theor. Biol.*, **231**, 525–533.
38. Rippe,K. (2001) Making contacts on a nucleic acid polymer. *Trends Biochem. Sci.*, **26**, 733–740.
39. Shimada,J. and Yamakawa,H. (1984) Ring-closure probabilities for twisted wormlike chains – applications to DNA. *Macromolecules*, **17**, 689–698.
40. Strahs,D. and Brenowitz,M. (1994) DNA Conformational-changes associated with the cooperative binding of CI-repressor of bacteriophage-lambda to O-R. *J. Mol. Biol.*, **244**, 494–510.
41. Purohit,P.K. and Nelson,P.C. (2006) Effect of supercoiling on formation of protein-mediated DNA loops. *Phys. Rev. E*, **74**.
42. Strick,T.R., Croquette,V. and Bensimon,D. (1998) Homologous pairing in stretched supercoiled DNA. *Proc. Natl Acad. Sci. USA*, **95**, 10579–10583.
43. Wang,M.D., Yin,H., Landick,R., Gelles,J. and Block,S.M. (1997) Stretching DNA with optical tweezers. *Biophys. J.*, **72**, 1335–1346.
44. Little,J.W., Shepley,D.P. and Wert,D.W. (1999) Robustness of a gene regulatory circuit. *EMBO J.*, **18**, 4299–4307.
45. Press,W.H., Teukolsky,S. A., Vettering,W.T. and Flannery,B.P. (1992) *Numerical Recipes in C*. Cambridge University Press. Cambridge, U.K. Chapter 15.6, pp. 692–694.